

**CONTENTS — A through E**

---

Experimental Constraints on Oxygen and Other Light Element Partitioning During Planetary Core Formation <i>C. B. Agee</i> .....	3021
In Situ Determination of Fe <sup>3+</sup> / Fe of Spinel by Electron Microprobe: An Evaluation of the Flank Method <i>J. Berlin, M. Spilde, A. J. Brearley, D. S. Draper, and M. D. Dyar</i> .....	3033
The Effect of Oxygen Fugacity on Large-Strain Deformation and Recrystallization of Olivine <i>M. Bystricky and K. Kunze</i> .....	3059
Plagioclase-Liquid Trace Element Oxygen Barometry and Oxygen Behaviour in Closed and Open System Magmatic Processes <i>D. Canil and J. Thom</i> .....	3016
Core Formation in the Earth: Constraints from Ni and Co <i>N. L. Chabot, D. S. Draper, and C. B. Agee</i> .....	3017
Oxygen Isotopic Compositions of the Terrestrial Planets <i>R. N. Clayton</i> .....	3020
The Effect of Oxygen Fugacity on Electrical Conduction of Olivine and Implications for Earth's Mantle <i>S. Constable, J. J. Roberts, and A. Duba</i> .....	3058
Redox Chemical Diffusion in Silicate Melts: The Impact of the "Semiconductor Condition" <i>R. F. Cooper</i> .....	3030
Ultra-High Temperature Effects in Earth's Magma Ocean: Pt and W Partitioning <i>E. Cottrell and D. Walker</i> .....	3046
Terrestrial Oxygen and Hydrogen Isotope Variations: Primordial Values, Systematics, Subsolidus Effects, Planetary Comparisons, and the Role of Water <i>R. E. Criss</i> .....	3037
Redox State of the Moon's Interior <i>J. W. Delano</i> .....	3008
How did the Terrestrial Planets Acquire Their Water? <i>M. J. Drake, M. Stimpfl, and D. S. Lauretta</i> .....	3043
Molecular Oxygen Mixing Ratio and Its Seasonal Variability in the Martian Atmosphere <i>C. England and J. D. Hrubes</i> .....	3009

**EXPERIMENTAL CONSTRAINTS ON OXYGEN AND OTHER LIGHT ELEMENT PARTITIONING DURING PLANETARY CORE FORMATION.** C. B. Agee, Institute of Meteoritics and Department of Earth and Planetary Sciences, University of New Mexico, Albuquerque NM 87131, agee@unm.edu.

**Introduction:** The nature of the light element content of the Earth's molten outer core has been actively debated since Birch [1] first proposed that some mix of light elements such as O, S, and Si could account for the apparent 10% density deficit there. Over the past several years numerous high-pressure experimental studies have placed important constraints on the physics and chemistry of planetary core formation. Based on siderophile element partitioning studies [2-4] core formation for the Earth appears to have occurred within a deep magma ocean. Thus the effects of pressure and temperature are important factors to consider in modelling the fate of light elements during core-mantle segregation. Here I review our current knowledge of oxygen, sulfur, and silicon partitioning between Fe-metal and silicate at extreme conditions, and the constraints these data place on light element behavior during planetary core formation.

**Oxygen:** Kato and Ringwood [5] performed some of the first exploratory partitioning experiments and suggested that a pressure effect would cause sufficient oxygen to dissolve into iron metal at the Earth's core-mantle boundary to account for the density deficit. More recent work by O'Neill et al. [6] and Rubie et al. [7] contradict Kato and Ringwood, showing that pressure actually decreases the solubility of oxygen with pressure. Li and Agee [8] and Rubie et al. [7] performed isobaric experiments up to 2673K and observed a strong positive temperature effect on  $D_{\text{O}}$  metal/silicate at constant  $f\text{O}_2$ . This result led Rubie et al. to propose that terrestrial planets of different size can end up with dramatically different core mass fractions and mantle iron oxide compositions – even if they formed from the same solar nebula or chondritic material. For example, this may be possible if the Earth's magma ocean was under higher pressure and thus hotter during core formation, while Mars' magma ocean had only modest pressures and temperatures.

**Sulfur:** Li and Agee [8] examined the effects of pressure and temperature on sulfur partitioning between molten iron-alloy and molten silicate in carbonaceous and ordinary chondrite starting materials up to 20 GPa and 2673K. Here pressure has a dramatic positive effect on  $D_{\text{S}}$  metal/silicate increasing from 74 to 533 over the pressure range 2-20 GPa at constant  $T=2273\text{K}$ . Temperature, on the other hand, decreases  $D_{\text{S}}$ . For example, over the range 2073-2623K, under isobaric conditions at 10 GPa,  $D_{\text{S}}$  decreases from 302 to 81. Even though the strong pressure effect is damped by an offsetting negative temperature effect,  $D_{\text{S}}$  is

expected to remain significantly greater than unity at all conditions of planetary core formation. Thus, sulfur may be one of the dominant light elements in the core if a sufficient quantity of it was sequestered in the Earth during accretion. Interestingly, the partitioning data indicate that the sulfur content of the upper mantle (250 ppm) is too high to have equilibrated with a molten outer core containing 2-10 wt% sulfur. Mass balance requires that additional sulfur be added to the upper mantle from other sources, possibly as part of a 0.2-0.6% Earth-mass late veneer.

**Silicon:** Li and Agee [8] found that temperature and pressure no have detectable effects on the partitioning of Si between Fe-metal and silicate in chondritic starting materials at  $f\text{O}_2$  ranging from the iron-wuestite (IW) buffer to 2 log units below IW. Under highly reducing conditions,  $D_{\text{Si}}$  has been shown to increase significantly [9,10], however for Si be the dominant light element in the core would require an  $f\text{O}_2$  of approximately log \_IW-4 to -6, much lower than is suggested by the Earth's core mass and FeO content of mantle xenoliths.

**References:** [1] Birch, F. J. *Geophys. Res.* 69, 4377-4388 (1964). [2] Li, J. & Agee, C.B. *Nature* 381, 686-689 (1996). [3] Li, J. & Agee, C.B. *Geochim. Cosmochim. Acta* 65, 1821-1832 (2001). [4] Chabot, N.L. & Agee, C.B. *Geochim. Cosmochim. Acta* 67, 2077-2091 (2003). [5] Kato, T. & Ringwood, A.E. *Phys. Chem. Minerals* 16, 524-538 (1989). [6] O'Neill, H.S.C., Canil, D. & Rubie, D.C. *J. Geophys. Res.* 103, 12,239-12,260 (1998). [7] Rubie, D.C., Gessmann, C.K. & Frost, D.J. *Nature* in press (2004). [8] Li, J. & Agee, C.B. *Geophys. Res. Lett.* 28, 81-84 (2001). [9] Kilburn, M.R. & Wood, B.J. *Earth Planet. Sci.* 152, 139-148 (1997). [10] Gessmann, C.K. & Rubie D.C. *Geochim. Cosmochim. Acta* 62, 867-882, (1998).

**IN SITU DETERMINATION OF  $\text{Fe}^{3+}/\Sigma\text{Fe}$  OF SPINELS BY ELECTRON MICROPROBE: AN EVALUATION OF THE FLANK METHOD.** J. Berlin<sup>1</sup>, M. Spilde<sup>2</sup>, A. J. Brearley<sup>1</sup>, D. S. Draper<sup>2</sup> & M. D. Dyar<sup>3</sup>. <sup>1</sup>Department of Earth & Planetary Sciences, University of New Mexico, Albuquerque, NM 87131, U.S.A., <sup>2</sup>Institute of Meteoritics, University of New Mexico, Albuquerque, NM 87131, U.S.A., <sup>3</sup>Department of Earth and Environment, Mount Holyoke College, South Hadley, MA 01075, U.S.A., E-mail: [jberlin@unm.edu](mailto:jberlin@unm.edu)

**Introduction:** In the past decade, progress has been made in the *in situ* determination of  $\text{Fe}^{3+}/\Sigma\text{Fe}$  ratios of minerals (which can be used to infer oxygen fugacity,  $f\text{O}_2$ ) with techniques such as TEM-EELS, Mössbauer milliprobe, and microXanes [1-3]. In addition, electron microprobes can measure the intensity change and shift of the L lines with the oxidation state of iron [4-7]. We are currently investigating potential applications of the Flank method [4-6] to geologic problems. Our goal is to evaluate whether the Flank method can be used to detect variation of  $\text{Fe}^{3+}/\Sigma\text{Fe}$  (and hence  $f\text{O}_2$ ) in spinel grains from terrestrial mantle xenoliths.

**Technique:** The Flank method [4-6] uses the differences between Fe L line spectra of Fe oxides with varying oxidation states (wüstite, magnetite, hematite) which are most pronounced on the low energy flank of the Fe L $\beta$  line and on the high energy flank of the Fe L $\alpha$  line. When X-ray intensities are determined at fixed wavelengths on the flanks of the L $\alpha$  and L $\beta$  peaks, the L $\beta/\text{L}\alpha$  intensity ratios are inversely correlated with the  $\text{Fe}^{3+}/\Sigma\text{Fe}$  ratios for the three pure Fe oxides. For these phases, an error as small as 0.02 for the  $\text{Fe}^{3+}/\Sigma\text{Fe}$  ratio is obtained [4]. However, for more complex minerals, matrix effects (chemical bonding and composition) affect the L $\beta/\text{L}\alpha$  ratio dramatically. To account for these matrix effects and before the method can be applied to minerals with unknown  $\text{Fe}^{3+}/\Sigma\text{Fe}$  ratios, working curves need to be established as was done for synthetic garnets by Höfer & Brey [6].

**Samples:** In order to investigate if a Flank-method calibration curve for spinels can be established, we are using samples with  $\text{Fe}^{3+}/\Sigma\text{Fe}$  ratios that have been determined previously by Mössbauer spectroscopy on bulk spinel separates. These include spinels from the Simcoe volcano, Washington [8], Cima and Dish Hill, California as well as from Harrat al Kishb and Harrat Hutaymah, Saudi Arabia. The Simcoe spinels have similar bulk compositions ( $\text{Mg}\# = 69.0\text{-}72.4$ ,  $\text{Cr/Cr+Al} = 31.9\text{-}34.5$ ) and range in  $\text{Fe}^{3+}/\Sigma\text{Fe}$  from 27 to 38. The other spinels show a wide range of compositions ( $\text{Mg}\# = 70.0\text{-}78.6$ ,  $\text{Cr/Cr+Al} = 9.8\text{-}32.2$ ) and have  $\text{Fe}^{3+}/\Sigma\text{Fe}$  from 12 to 37.

We are also analyzing xenolith samples from the Puerco Necks, New Mexico, for which Mössbauer data have not been obtained yet. Spinels in these samples are especially likely to have variations of  $\text{Fe}^{3+}/\Sigma\text{Fe}$  on the microscopic scale as they show compositional zoning

in addition to exhibiting a wide range of colors (brown, black, green, and purple).

**Preliminary results:** The calibration of the Flank method for spinels is complicated by many factors such as the huge range of compositional, structural, and bonding effects which can change the shape of the Fe L lines. In addition, instrumental parameters such as spectrometer reproducibility [5] and stability of the beam current during the measurements need to be monitored carefully. Keeping the beam current constant ( $50.0 \pm 0.2$  nA), we have found significant variations in the shapes of Fe L spectra taken on single spinel grains of Puerco neck xenoliths (Fig. 1). However, these variations are not systematic in a way that would imply core-to-rim zoning in  $\text{Fe}^{3+}/\Sigma\text{Fe}$  and thus  $f\text{O}_2$ .

**Acknowledgements:** We are grateful to A. Brandon and J. Selverstone, who are providing samples for this study.

**References:** [1] Garvie L. A. J. & Buseck P. R. (1998) *Nature* **396**, 667-670. [2] Sobolev V. N. et al. (1999) *Am. Min.* **84**, 78-85. [3] Delaney J. S. et al. (1998) *Geology* **26**, 139-142. [4] Höfer H. E. et al. (1994) *Europ. J. Min.* **6**, 407-418. [5] Höfer H. E. et al. (2000) *Europ. J. Min.* **12**, 63-71. [6] Höfer H. E. & Brey G. P. (2001) *11th Ann. Goldschmidt Conference*, # 3227. [7] Fialin M. et al. (2001) *Am. Min.* **86**, 456-465. [8] Brandon A. D. & Draper D. S. (1996) *GCA* **60**, 1739-1749.

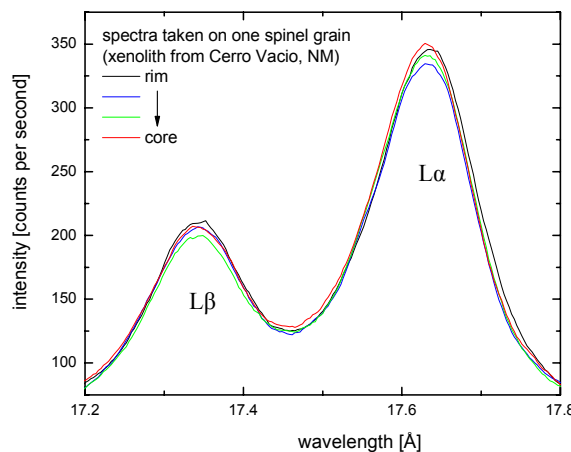


**Fig. 1:** Fe L emission spectra taken on one spinel grain in a xenolith sample from Cerro Vacío, NM (10 keV, 50 nA, TAPJ crystal). The spectra are smoothed.

**THE EFFECT OF OXYGEN FUGACITY ON LARGE-STRAIN DEFORMATION AND RECRYSTALLIZATION OF OLIVINE.** M. Bystricky and K. Kunze. Geologisches Institut, ETH Zürich, Sonneggstrasse 5, CH-8092 Zürich, Switzerland.**Abstract:**

The rheological properties of olivine, the most abundant phase in the Earth upper mantle, are likely to govern mantle dynamics. In particular, the development of crystallographic preferred orientations (CPOs) in olivine during deformation and recrystallization gives rise to seismic anisotropy in the mantle. Recent experimental studies have shown that different CPOs develop at large strains for dry olivine [1-2], wet olivine [3] and olivine with melt [4]. In this study, we have focused on the effect of oxygen fugacity on the deformation and recrystallization of dry olivine.

Large-strain deformation experiments were performed on hot-pressed polycrystalline olivine aggregates under conditions (temperature, pressure, strain rate and grain size) favoring dislocation creep. Cylindrical samples were deformed in torsion in a gas-medium apparatus at 1200-1300°C, a confining pressure of 300 MPa and constant twist rates corresponding to constant shear strain rates of  $5 \cdot 10^{-5}$  to  $3 \cdot 10^{-4}$  s $^{-1}$  at the samples' outer diameters. The oxygen fugacity was controlled by placing the samples in an iron or a nickel sleeve, yielding oxygen fugacities near the iron-iron wüstite (Fe/FeO) or the nickel-nickel oxide (Ni/NiO) phase boundaries, respectively. Simple shear microstructures were observed by light microscopy and CPOs were analysed by orientation mapping using electron backscatter diffraction.

The strength of dry polycrystalline olivine is weakly dependent on oxygen fugacity. At low strain, peak stress values (at both Ni/NiO and Fe/FeO) are very consistent with previous rheological data on dislocation creep of olivine obtained in coaxial experiments under dry conditions [5-6]. Microstructures show evidence for dislocation creep and recovery in the form of deformation lamellae and subgrains. A typical deformation texture with [100] axes oblique to the shear direction is present at shear strains of  $\sim 0.5$ .

After the initial peak stress, significant weakening occurs with increasing shear strain ( $\gamma \sim 0.3-3$ ). Weakening becomes less important at larger strains and stress seems to approach a steady value at shear strains of  $\gamma \sim 6-8$ . The total weakening at large strains is approximately 20-40%. The determination of stress exponents of about 3-3.5 at various finite strains and of strong CPOs in all deformed samples suggest that dis-

location creep processes remain dominant throughout the experiments.

Microstructural observations of samples deformed at Fe/FeO and 1200-1250°C indicate continuous dynamic recrystallization mainly by subgrain rotation and some grain boundary migration. Recrystallization is accompanied by important grain refinement and leads to strongly foliated microstructures. With increasing temperature, grain boundaries become much more mobile. At 1300°C recrystallization occurs mainly by grain boundary migration, producing microstructures with a less pronounced foliation. At all temperatures, a strong recrystallization CPO in highly deformed samples is characterized by alignment of [100] in the shear direction and girdles of [010] and [001] approximately normal to that direction. This texture is interpreted as due to dislocation glide on several {0kl}[100] slip systems, including activation of (010)[100].

At Ni/NiO, recrystallization is more efficient and seems to be dominated by grain boundary migration. Straight and parallel grain boundaries are often aligned across several grains, suggesting some contribution of grain boundary sliding at large strains, possibly assisted by diffusion processes. A strong CPO with [100] aligned in the shear direction and a [010] point maximum perpendicular to the shear plane suggest dislocation creep primarily on the (010)[100] slip system.

Our study shows that during large strain deformation and recrystallization of dry olivine in the dislocation creep regime, more oxidizing conditions promote diffusion processes and grain boundary sliding. Although the presence of a strong CPO suggests that dislocation creep remains active at large strains, grain boundary sliding processes may accommodate some of the strain leading to a de-emphasis of stronger slip systems in olivine in favor of dominant slip on the single (010)[100] slip system.

**References:** [1] Zhang S. and Karato S. (1995) *Nature* 375, 774-777. [2] Bystricky M. et al. (2000) *Science* 290, 1564-1567. [3] Jung H. and Karato S. (2001) *Science* 293, 1460-1463. [4] Holtzman B.K. et al. (2003) *Science* 301, 1227-1230. [5] Karato S. et al. (1986) *J. Geophys. Res.* 91, 8151-8176. [6] Mei S. and Kohlstedt D.L. (2000) *J. Geophys. Res.* 105, 21471-21481.

**PLAGIOCLASE-LIQUID TRACE ELEMENT OXYGEN BAROMETRY AND OXYGEN BEHAVIOUR IN CLOSED AND OPEN SYSTEM MAGMATIC PROCESSES.** Dante Canil<sup>1</sup> and James Thom<sup>2</sup> <sup>1</sup>School of Earth and Ocean Sciences, University of Victoria, Victoria, B.C., Canada, dcanil@uvic.ca <sup>2</sup>Department of Earth and Ocean Sciences, University of British Columbia, Vancouver, B.C..

**Introduction:** There are several measurements of the oxygen fugacity recorded by magmas, and related concern about the behaviour of oxygen in magmas. Do magmas exchange oxygen in an open process through homogeneous equilibria, or do they remain closed systems along their liquid line of descent? Evidence for mixing of several magma batches in many magma types suggests truly open systems, and many oxygen barometers record crystallization along or parallel to ‘buffers’ such that the magma must exchange oxygen or ‘breathe’ by interaction with a separate redox reservoir, likely sulfur [1].

In this study, we explore the use of trace element signatures in plagioclase as an indicator of the oxygen fugacity recorded by magmas with multiple histories, or by extraterrestrial samples. Plagioclase is a ubiquitous mineral in magmas ranging in composition from basalt to rhyolite, and often shows a detailed record of the magma batches into which it has been mixed and recycled. We experimentally calibrate the partition of redox sensitive elements (V, Mn) into plagioclase with a view to using concentration profiles for these elements to infer conditions of oxygen fugacity during crystallization, mixing, resorption and recycling, or as an empirical oxygen barometer in many terrestrial and extraterrestrial samples for which no other traditional methods can be employed.

**Methods:** Experiments were performed at 100 kPa in synthetic (Di-Ab-An) and natural systems (MORB, alkali basalt) in a vertical tube furnace, with fO<sub>2</sub> fixed by CO – CO<sub>2</sub> gas mixing. Natural basalts were crystallized between 1200 and 1150°C at fO<sub>2</sub> conditions of about one to four log units below the nickel-bunsenite (NNO) buffer (NNO-1 to NNO-4). Cooling histories were used to produce large plagioclase grains (300 microns) and glass for analysis by laser ablation inductively coupled plasma mass spectrometry (LA ICP MS). Charges were mounted on Re ribbon or pre-saturated Pt wire loops, to avoid Fe loss. Some experiments were ‘reversed’ by approaching final conditions from both low and high fO<sub>2</sub>.

**Results:** Over an increase in fO<sub>2</sub> of only 2 log units (NNO-3.5 to NNO-1.5), Mn and V concentrations in plagioclase decrease from 600 to 30 ppm, and from 150 to 5 ppm, respectively. Liquid composition is constant in Mn (~ 1300 ppm) and V (~ 250 ppm) in all

experiments. The resultant partition coefficients, DMn and DV (plag/liq) are similar and vary from ~ 0.4 to ~0.02 between NNO-3.5 to NNO-1.5. The changes in DMn and DV with fO<sub>2</sub> are thus dominated by substitution into the crystal. The D(plag/liq) for Ga, REE, Mg, Ca, Ba, and Sr were also determined by LA ICP MS in the same experiments. Onuma diagrams (logD element vs. ionic radius) show that Mn enters plagioclase principally as Mn<sup>2+</sup>. The case is less clear for V<sup>2+</sup>. The large changes in D plag/liq for these elements with increasing oxygen fugacity are due to less Mn<sup>2+</sup> (or V<sup>2+</sup>) available in the liquid for substitution into plagioclase.

We apply our partitioning data in a preliminary way to mid-Atlantic MORB and arc basalts from the Kuriles and from Mt. Adams, Washington. We obtain fO<sub>2</sub>'s of NNO-2.5 and NNO-1, respectively, consistent with previous measurements and with ‘conventional wisdom’. Current applications in progress are to unravel the redox history recorded by zoned plagioclase in erupted rocks from mid-ocean ridges, Mt. St. Helens, Washington, and Mt. Meager, British Columbia. Coupled with these experimental results, the growing use of trace element microanalysis in petrology should provide further constraints on the detailed behaviour of oxygen during the crystallization, mixing and eruption of any terrestrial or extraterrestrial magma having plagioclase on its liquidus.

**References:**

- [1] Carmichael and Ghiorso, 1986, EPSL, 78, 200-210.

**CORE FORMATION IN THE EARTH: CONSTRAINTS FROM NI AND CO.** N. L. Chabot<sup>1</sup>, D. S. Draper<sup>2</sup>, and C. B. Agee<sup>2</sup>, <sup>1</sup>Dept. of Geology, 112 A. W. Smith Bldg., Case Western Reserve University, Cleveland, OH, 44106-7216. nlc9@po.cwru.edu. <sup>2</sup>Institute of Meteoritics, Department of Earth and Planetary Sciences, University of New Mexico, Albuquerque, NM, 87131-1126.

Due to their metal-loving nature, Ni and Co were strongly partitioned into the metallic core and were left depleted in the silicate mantle during core formation in the Earth. Based on experimental liquid metal-liquid silicate partition coefficients (D), studies have suggested that core formation in an early magma ocean can explain the observed mantle depletions of Ni and Co [1-5]. However, the conditions proposed by the magma ocean models have ranged from pressures of 24 to 59 GPa and temperatures of 2200 to < 4000 K. Furthermore, the proposed magma ocean oxygen fugacities have differed by nearly two orders of magnitude, from 0.4 to 2.2 log units below the iron-wüstite buffer ( $\Delta\text{IW} = -0.4$  to -2.2).

Chabot and Agee [6] noted that the different models predicted contradictory behaviors for D(Ni) and D(Co) as a function of temperature. With the hope of resolving the discrepancies between the magma ocean models, we conducted a systematic experimental study to constrain the effects of temperature on D(Ni) and D(Co). Our preliminary multi-anvil experimental results are shown in Fig. 1.

Combining our temperature results with the well-determined effects of pressure from previous studies [e.g. 1, 5] and treating Ni and Co as divalent [e.g. 7], we have parameterized D(Ni) and D(Co) as functions of pressure, temperature, and oxygen fugacity, using a mathematical form similar to previous work [2-5]. For compositions appropriate to the Earth's core, the effects of S and C on D(Ni) and D(Co) are small [6, 8], as are the effects from silicate composition [9].

Using our parameterizations, we can get pressure, temperature, and oxygen fugacity solutions where D(Ni) and D(Co) are both within a factor of two of the partition coefficients needed to explain the mantle depletions by core formation in a magma ocean. Figure 2 shows the solution spaces for two different oxygen fugacities proposed by the magma ocean models. Surprisingly, despite very different predicted effects of temperature by the models, all of the previous models fall in one of our determined solution spaces. Thus, our work shows the proposed conditions are all mathematically possible. However, if the FeO content of the mantle is used as an additional constraint, the oxygen fugacity suggested by core-mantle equilibrium is about -2.2  $\Delta\text{IW}$ , supporting core formation in a magma ocean at 40 to 60 GPa and a temperature > 2500 K.

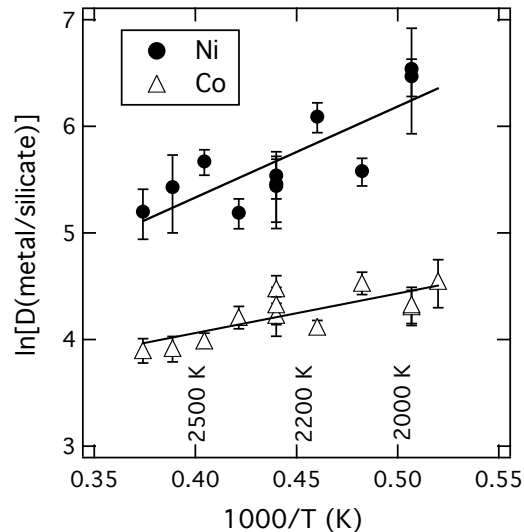


**Fig. 1.** Experimental data at 7 GPa with 2% errors, corrected to a common oxygen fugacity of -1.5  $\Delta\text{IW}$ .

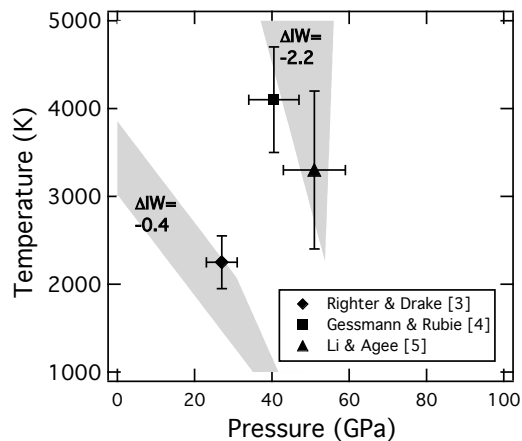


**Fig. 2.** The two shaded areas show the solution spaces for oxygen fugacities of -0.4 and -2.2  $\Delta\text{IW}$ , where our parameterized D(Ni) and D(Co) both fall within a factor of two of the needed values.

- References:** [1] Li J. and Agee C. B. (1996) *Nature* 381, 686-689. [2] Righter K. et al. (1997) *PEPI* 100, 115-134. [3] Righter K. and Drake M. J. (1999) *EPSL* 171, 383-399. [4] Gessmann C. K. and Rubie D. C. (2000) *EPSL* 184, 95-107. [5] Li J. and Agee C. B. (2001) *GCA* 65, 1821-1832. [6] Chabot N. L. and Agee C. B. (2002) *LPS XXXIII*, #1009. [7] Holzheid A. et al. (1994) *GCA* 58, 1975-1981. [8] Chabot N. L. et al. (2003) *MAPS* 38, 181-196. [9] Jana D. and Walker D. (1997) *EPSL* 150, 463-472. [10] NASA grants NAG5-12831 and 344-31-20-25.

**OXYGEN ISOTOPIC COMPOSITIONS OF THE TERRESTRIAL PLANETS.** Robert. N. Clayton, Enrico Fermi Institute, University of Chicago, Chicago, IL 60637, USA. r-clayton@uchicago.edu

Mechanisms that may account for oxygen isotope heterogeneity in meteorites on the microscopic scale do not seem adequate for explaining the similarities and differences in isotopic composition on a planetary scale. In chondrites, most of the isotopic variability can be attributed to photochemical enrichment of the two rare heavy isotopes with respect to the  $^{16}\text{O}$ -rich solar composition [1]. In the CO, CM, CI, and CR chondrites, an additional low-temperature aqueous alteration leads to mass-dependent further enrichment of the heavy isotopes.

If the proposed origin of the isotopic variation in chondrites is correct, then only a small fraction, represented primarily in CAIs, has the solar oxygen isotopic composition, and all other meteoritic components must have undergone photochemical processing. In addition, since the bulk isotopic compositions of the terrestrial planets and of the achondrite parent bodies are similar to those of chondrites, they too must be made of photochemically enriched matter. The photochemical reactions produce a non-equilibrium assemblage of gases, probably leading to a non-equilibrium assemblage of solids, particularly with respect to their oxidation state. These issues emphasize the importance of the measurement of oxygen isotopes in the Genesis solar wind mission.

Within the Earth, oxygen isotope variations are due almost entirely to mass-dependent fractionation effects, giving a line of slope 0.52 on the three-isotope plot. The average crustal composition is 3–4‰ higher in  $\delta^{18}\text{O}$  than the upper mantle. This difference is too large to be due to igneous fractionation effects alone, and reflects the larger, low-temperature iso-

tope fractionation associated with aqueous weathering reactions at the Earth's surface. Similar effects are not observed in the intraplanetary isotopic variations in the Moon or in the parent bodies of the HED and SNC meteorites.

The bulk oxygen isotopic compositions of Earth and Mars (assumed to be the SNC parent body) cannot be accounted for by any mixture of two components, such as those proposed by Ringwood [2] and Wänke [3]. In principle, three-component mixtures of ordinary chondrites, CI, and CV chondrites can match the planetary isotopic compositions, but are inconsistent with chemical compositions. An additional unexplained observation is the exact coincidence in oxygen isotopic composition between Earth and Moon. The correspondence of isotopic composition between the Earth and the enstatite chondrites has been taken by some to have direct genetic significance [4]. In all models using primitive chondrites as building blocks for the terrestrial planets, there is a necessity to remove a major fraction of the moderately volatile elements (alkalies, S, etc.), without altering their isotopic compositions [5].

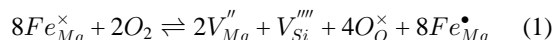
**References:** [1] Clayton R. N. (2002) *Nature*, 415, 860–861. [2] Ringwood A. E. (1979) *Composition and Origin of the Earth*, RSES, Aust. Nat. Univ. (65 pp.). [3] Wänke H. (1981) *Phil. Trans. Roy. Soc. Lond.*, A303, 287–302. [4] Javoy M. (1995) *Geophys. Res. Lett.*, 22, 2219–2222. [5] Humayun M. and Clayton R. N. (1995) *Geochim. Cosmochim. Acta*, 59, 2131–2148.

**THE EFFECT OF OXYGEN FUGACITY ON ELECTRICAL CONDUCTION IN OLIVINE AND IMPLICATIONS FOR EARTH'S MANTLE.** S. Constable<sup>1</sup>, J.J. Roberts<sup>2</sup>, and A. Duba<sup>3</sup>. <sup>1</sup>Scripps Institution of Oceanography, La Jolla, CA 92093-0225, sconstable@ucsd.edu. <sup>2</sup>Lawrence Livermore National Laboratory, Livermore, CA 94551, roberts17@llnl.gov. <sup>3</sup>American Museum of Natural History, New York, NY 10024-5192, duba@amnh.org.

**Abstract:** Because electrical conductivity is exponentially dependent on temperature and also a function of composition and phase, studies of mantle conductivity have long held the promise of providing information on the thermal and compositional state of Earth's mantle. Two techniques for probing deep conductivity exist; the magnetotelluric (MT) method of recording surface magnetic and electric fields, and the geomagnetic depth sounding (GDS) method of separating externally generated and internally induced magnetic fields from vector magnetometer records. The GDS method has recently gained momentum from the application of magnetic satellite data, which provide a global coverage not possible using land-based observatories alone [1].

The bridge between these field studies and the internal constitution of Earth is provided by laboratory measurements of Earth materials as a function of temperature, composition, and pressure. Oxygen fugacity  $f_{O_2}$  plays many important roles in this enterprise. First and foremost,  $f_{O_2}$  must be controlled sufficiently to keep the sample within its stability field, or irreversible changes in composition and conductivity occur [2]. Secondly, electrical conductivity of olivine, and presumably other mantle materials in which iron influences conductivity and stoichiometry, depends on  $f_{O_2}$  and the oxidation state of the mineral. Thirdly,  $f_{O_2}$  can be used as a laboratory tool for probing the behavior of defects in mantle minerals.

We have studied the effect of oxygen on the electrical properties of olivine,  $(Mg_{0.9}Fe_{0.1})_2SiO_4$ , the dominant mineral of Earth's upper mantle, in an effort to quantitatively describe conduction mechanism, charge mobility, and defect concentration. The working model for the relationship between the major defect populations and  $f_{O_2}$  is described by



[3,4] with magnesium vacancies  $V_{Mg}''$  and polarons (holes localized on  $Fe_{Mg}^{\bullet}$ ) both candidates for dominant conduction defects. Room pressure electrical conductivity as a function of temperature and  $f_{O_2}$  demonstrates an increase in conductivity with both parameters, representing the combined effects of increased mobility, increased defect concentration, and shifting conduction mechanism. The addition of thermopower measurements, in which the electric field generated by a temperature gradient is measured, allows one to separate the mobility term from concentration. A mathematical model describing conductivity and thermopower as a function of mobility, concentration, and defect type is inverted to obtain separate estimates of the defect concentrations [ $V_{Mg}''$ ] and [ $Fe_{Mg}^{\bullet}$ ] as well as their mobilities [5]. The contribution of these defects to electrical conduction in olivine, and thus presumably the mantle, varies by nearly an order of magnitude as  $f_{O_2}$  spans the stability field.

In an independent experiment, the exponential change in conductivity after an abrupt change in  $f_{O_2}$  external to the sample can be used to estimate the diffusivity, and thus mobility, of defects responsible for chemical re-equilibration [6]. Again, an extensive data set of relaxation times as a function of  $f_{O_2}$  and temperature was modeled to extract mobility as a function of temperature for multiple defect species. The mobilities of the two species required by the re-equilibration data agrees extremely well with the mobilities for  $V_{Mg}''$  and  $Fe_{Mg}^{\bullet}$  derived from the thermopower modeling, suggesting that these conductive species are also responsible for the rate of the defect reaction (1). The agreement (shown in Fig. 1) between the two different methods (thermopower modeling and  $f_{O_2}$  re-equilibration) carried out on two different samples (San Quintin dunite and Mt. Porndon lherzolite) suggests that the mobilities derived for these defects are reliable.

Although many uncertainties and unconstrained variables remain in our efforts to characterize mantle conductivity (for example, the role of hydrogen/water in conduction), it is clear that the effect of oxygen cannot be ignored when interpreting field measurements using laboratory data sets.

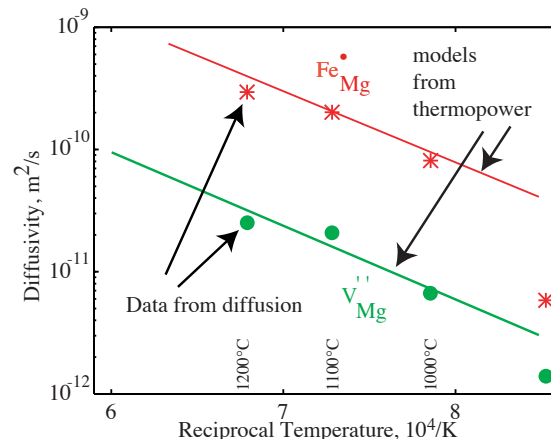


Figure 1: Diffusivities for  $V_{Mg}''$  and  $Fe_{Mg}^{\bullet}$  derived from thermopower mobilities (lines) and  $f_{O_2}$  re-equilibration (symbols) as a function of temperature.

## References:

- [1] Constable, S., and Constable, C. (2004) *Geochem. Geophys. Geosys.*, 5 10.1029/2003GC000634.
- [2] Duba, A., and Nicholls, I.A. (1973) *Earth Planet. Sci. Lett.* 18 59–64.
- [3] Smyth, D.M., and Stocker, R.L. (1975) *Phys. Earth Planet. Int.* 10 183–192.
- [4] Schock, R.N., Duba, A., and Shankland, T.J. (1989) *J. Geophys. Res.* 94 5829–5839.
- [5] Constable, S., and Roberts, J.J. (1997) *Phys. Chem. Min.* 24 319–325.
- [6] Constable, S., and Duba, A. (2002) *Phys. Chem. Min.* 29 446–454.

**REDOX CHEMICAL DIFFUSION IN SILICATE MELTS: THE IMPACT OF THE “SEMICONDUCTOR CONDITION.”** Reid F. Cooper, Department of Geological Sciences, Brown University, Providence, RI 02012–1846 USA (Reid\_Cooper@Brown.edu).

**Introduction:** Transition-metal-cation redox experiments designed to characterize the rate of oxygen-species diffusion in silicate melts reveal a startling result: for melts of similar polymerization, chemical diffusion seems to occur some  $10^2$ – $10^3$  times faster than that seen for  $^{18}\text{O}$  in tracer diffusion experiments [1–3]. The primary reason for the discrepancy is that, in many cases, the chemical diffusion producing the valence-state change of transition-metal cations does not involve diffusion of an oxygen species at all, but rather is wrought by the diffusion of network-modifying cations whose motion is decoupled from that of other ions by the high transport coefficient of electronic defects, i.e., electron holes ( $\text{h}^\bullet$ ) and/or electrons in the conduction band ( $e'$ )—a situation known as the “semiconductor condition” in chemical kinetics [4]. Cation-diffusion-effected redox reactions, in both melts and minerals, create reaction morphologies with implications, e.g., for the perceived chemistry of planetary surfaces and for the structures of metal-bearing chondrules.

**Oxidation of basaltic magmas:** Ion backscattering spectrometry was used to prove unequivocally (i.e., the reaction morphology is unique) that the physical process of oxidation of a basaltic liquid occurs, for anhydrous conditions, according to the dynamic shown in Fig. 1a [5]. When the external oxygen fugacity ( $f_{\text{O}_2}$ ) exceeds the magnetite-hematite (MH) buffer, two internal reaction fronts move into the melt:  $\xi'''$  is the location where the local  $f_{\text{O}_2}$  finally sees the melt go subliquidus, and magnetite nucleates;  $\xi''$  is the MH buffer, where the magnetite formed in the first (crystallization) reaction is converted to hematite. The process is accomplished by the flux ( $j_i$ ) of network-modifier  $\text{Fe}^{2+}$  and  $\text{Ca}^{2+}$  to the free surface, where they form thin-film oxides that coat the surface. The cation flux is charge-compensated by a counterflux of  $\text{h}^\bullet$ . For  $f_{\text{O}_2}$  conditions lower than MH but sufficiently high to intersect the liquidus, only the single reaction front  $\xi'''$  moved into the melt, and very little  $\text{Ca}^{2+}$  is mobilized; thus  $x$  in the figure approaches unity and  $y \ll x$ . The thin-film oxide is seen naturally as the multicolored specular patina on fresh basalt flows [e.g., 6], the color variation being a function of the film thickness. Reflectance spectroscopy on these surfaces clearly would reveal a  $\text{Fe}^{2+,3+}$  content exceeding greatly that of the bulk magma. The cation-diffusion-dominated oxidation response was proven to occur for  $\text{Fe}^{2+,3+}$  concentrations as low as 0.04 at% [7].

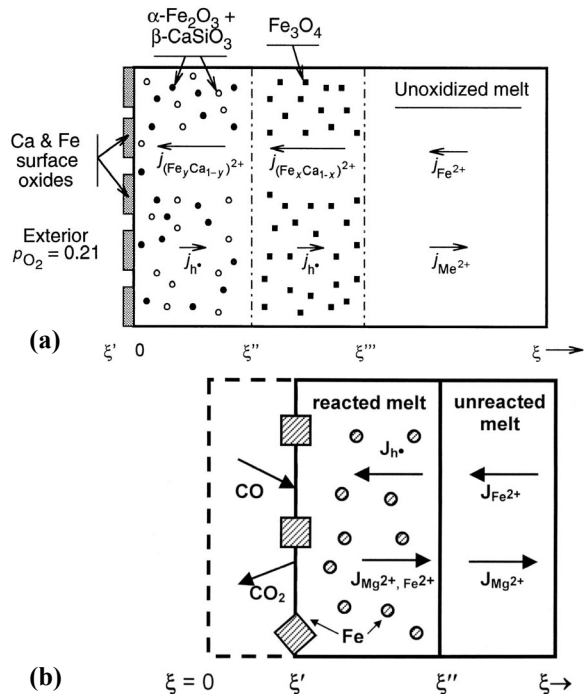


**Figure 1.** Redox dynamics in  $\text{Fe}^{2+,3+}$ -bearing silicate melts. **(a)** Oxidation in a basaltic melt. **(b)** Reduction in an Fe-MAS melt. Cation-diffusion-effected reactions are possible because of the flux of electron holes.

**Reduction of iron-oxide-bearing melts:** Experiments on  $\text{Fe}^{2+}$ -doped magnesium aluminosilicate (Fe-MAS) melts demonstrated the reduction dynamic depicted in Fig. 1b [8]: oxygen chemically ablates from the free surface and network-modifying cations diffuse inward, charge-compensated by a counterflux of  $\text{h}^\bullet$ ; nm-scale crystals of  $\alpha\text{-Fe}$  nucleate at an internal front,  $\xi''$ . Dispersal of iron grains suggests that the melt structure includes percolation of network modifiers. Surface iron crystals are affected by vapor-phase transport of iron. Lowering the  $f_{\text{O}_2}$  further, via increase in CO content of environment, sees a mechanism change to one in which a carbon species diffuses inward.

- [1] Dunn T. (1986) In *Silicate Melts*, Mineral. Soc. Canada, pp. 57–92.
- [2] Cook G.B. et al. (1990) *J. Non-Crys. Solids*, 120, 207–222.
- [3] Chakraborty S. (1995) *RiMG*, 32, 411–503.
- [4] Schmalzried H. (1981) *Solid State Reactions (2<sup>nd</sup> Edition)*, Verlag Chemie, p.99.
- [5] Cooper R.F. et al. (1996) *Science*, 274, 1173–1176.
- [6] Dutton C.E. (1884) In *USGS 4<sup>th</sup> Annual Report*, pp.75–219.
- [7] Cook G.B. and Cooper R.F. (2000) *Am. Mineral.*, 85, 397–406.
- [8] Everman R.L.A. and Cooper R.F. (2003) *J. Am. Ceram. Soc.*, 86, 487–494.

## ULTRA-HIGH TEMPERATURE EFFECTS IN EARTH'S MAGMA OCEAN: Pt and W PARTITIONING.

E.. Cottrell and D. Walker, <sup>1</sup>Lamont-Doherty Earth Observatory of Columbia University. Rt. 9W Palisades, NY 10964. [liz@ldeo.columbia.edu](mailto:liz@ldeo.columbia.edu) and [dwalker@ldeo.columbia.edu](mailto:dwalker@ldeo.columbia.edu)

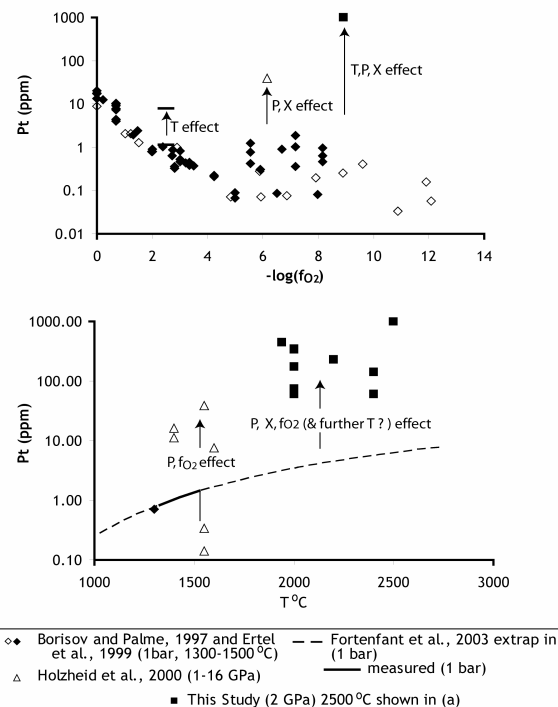
**Abstract:** New experiments to 2600°C (at 2 GPa, reducing conditions, at ~constant relative  $f_{O_2}$ ) demonstrate a very strong negative dependence of  $D_{Pt}^{met/sil}$ , and a weak negative dependence of  $D_W^{met/sil}$  on T. The Pt results reconcile mantle Pt abundances with the magma ocean model as suggested by [1], and also resolve the “nugget problem.” The W results allow hotter magma oceans to be compatible with mantle W abundance than if  $D_W^{met/sil}$  had a positive T dependence.

**Methods:** Ca-doped LaCrO<sub>3</sub> cylinders insulate short graphite (C) heaters from BaCO<sub>3</sub> piston cylinder pressure media while Mo-wrapped MgO spacers at either end of the C heaters insulate the piston and complete the electrical circuit. Experiments remain stable for 1-10 hours at T 2000-2600°C. For Pt experiments, a C capsule holds a small Pt clipping at the base of non-convecting, initially Pt-free silicate [2]. We initially used C capsules for W-silicate experiments; however, this resulted in prolific growth of metal carbides that rapidly (< 4 min at T ≥ 2000°C) established new equilibria. C capsules were replaced with pure W capsules for experiments on W solubility.

**Results for Pt:** At temperatures in excess of 2000°C silicate melt dissolves tens to hundreds of ppm Pt by weight – levels analyzed by EMP. Rapid quench results in concentric textural zones: the outermost (in contact with the C) is completely free of the micronuggets which have plagued previous investigations [3-5]. Interior regions of the silicate, which cooled more slowly, formed nuggets; however, the measured Pt concentration in the charge is spatially invariant. In addition, nugget size correlates with quench rate and is independent of run time. These observations in concert with the precautions taken by [2] strongly suggest a quench origin for Pt micronuggets. We measure  $D_{Pt}^{met/sil} \sim 10^3$ , 4-12 orders of magnitude lower than extrapolations from high  $f_{O_2}$ , 1 bar experiments at ≤ 1550°C [3-6] but consistent with measured Pt concentrations from [7], though our interpretations differ.

**Results for W:** Between 1450 and 2400°C in W capsules, holding silicate melt composition and relative  $f_{O_2}$  approximately constant,  $D_W^{met/sil}$  shows a small range of 60-100, in contrast to changes of many orders of magnitude found when composition and  $f_{O_2}$  vary [8-12]. C capsules form carbides above 1600°C. W concentration in the silicate plummets because

$D_W^{carbide/sil} \gg D_W^{met/sil}$ . If this process affected the high-T study of [10], the apparently higher  $D_W^{met/sil}$  of [10] compared to studies at moderate T are explained. Multiple linear regressions [e.g. 13] edited to remove the data of [10] should give decreasing  $D_W^{met/sil}$  (instead of increasing) as T increases! If  $D_W^{met/sil}$  did increase with T, only unrealistically cool magma oceans could dissolve the present mantle W abundances. This difficulty is removed with exclusion of the carbide-biased data.



### References:

- [1] Murthy V.R. (1991) Science, **253**: p. 303-306.
- [2] Cottrell E. and Walker D. (2002) 33<sup>rd</sup> LPSC, Abs no. **1274**.
- [3] Borisov A. and Palme H. (1997) GCA, **61**: p. 4349-4357.
- [4] Ertel W., et al. (1999) GCA, **63**: p. 2439-2449.
- [5] O'Neill H.S.C., et al. (1995) Chem Geol, **120**: p. 255-273.
- [6] Fortenfant S.S., et al. (2003) GCA, **67**: p. 123-131.
- [7] Holzheid A., et al. (2000) Nature, **406**: p. 396-399.
- [8] Jana D. and Walker D. (1997) EPSL, **150**: p. 463-472.
- [9] Jaeger W.L. and Drake M.J. (2000) GCA, **64**: p. 3887-3895.
- [10] Walter M.J. and Thibault Y. (1995) Science, **270**: p. 1186-1189.
- [11] Righter K. and Shearer C.K. (2003) GCA, **67**: p. 2497-2507.
- [12] Ertel W., et al. (1996) GCA, **60**: p. 1171-1180.
- [13] Righter K., et al. (1997) Phys Earth Planet Int, **100**: p. 115-134.

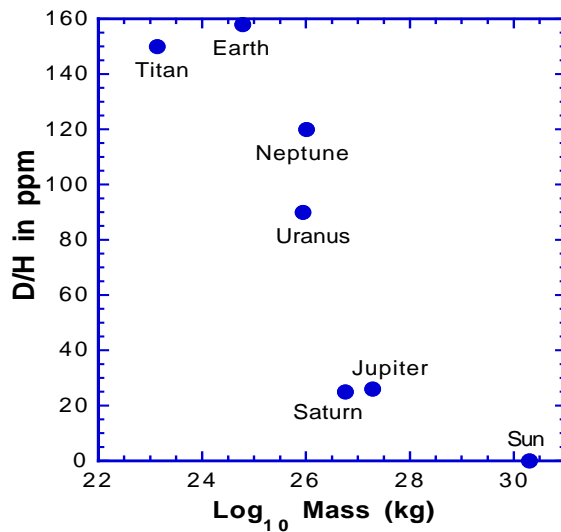
## TERRESTRIAL OXYGEN AND HYDROGEN ISOTOPE VARIATIONS: PRIMORDIAL VALUES, SYSTEMATICS, SUBSOLIDUS EFFECTS, PLANETARY COMPARISONS, AND THE ROLE OF WATER

Robert E. Criss, Washington University, St. Louis, MO 63130 criss@wustl.edu

**Introduction:** O and H isotopic variations provide key information on planetary formation and the evolution and interactions of their lithospheres, atmospheres and hydrospheres. Earth is best understood. The  $\delta^{18}\text{O}$  values of Earth's major lithospheric reservoirs such as MORB closely approximate those of lunar igneous rocks ( $+5.7 \pm 0.3\text{ ‰}$ ). This similarity suggests that Earth and Moon have a common primordial affinity and that  $+5.7\text{ ‰}$  is the bulk  $^{18}\text{O}$  composition in the Earth-Moon system, but only Earth's outermost layers have been sampled. Also, large total  $^{18}\text{O}$  ranges are observed for terrestrial magmas (-2 to  $+16\text{ ‰}$ , ref [1]), igneous rocks (-10.5 to  $+16\text{ ‰}$ ), and sedimentary rocks (at least -4 to  $+39\text{ ‰}$ ). Only small effects (< 2‰) can be attributed to pure fractional crystallization as isotopic fractionations are small at high temperatures; this partly explains why felsic rocks are systematically higher in  $^{18}\text{O}$  by 1-4 per mil than mafic and ultramafic rocks, but cannot explain the total ranges in terrestrial rocks. Earth's great ranges therefore require interaction or exchange of rocks and magmas with oxygen reservoirs at or near Earth's surface, where large enrichments or depletions in  $^{18}\text{O}$  are possible because fractionation factors are large at low temperatures. Key identified processes include aqueous deposition, subsolidus exchange with infiltrating hydrothermal fluids, and exchange with or assimilation of wallrocks having disparate compositions. Open and closed subsolidus processes are easily distinguished on  $\delta$ - $\delta$  plots, as they respectively create positive and negative-sloped trends in most cases [2]. Meteorites commonly feature pronounced disequilibrium effects but rarely show trends suggesting that coherent suites underwent subsolidus exchange.

The  $\delta\text{D}$  values of most sedimentary, metamorphic and igneous rocks on Earth are -40 to  $-95\text{ ‰}$ , a similarity indicating that subduction of hydrous sediments, followed by dehydration and recycling, has considerably homogenized the D/H ratio of Earth's outer layers [1]. These rock reservoirs plus the huge hydrosphere together comprise Earth's hydrogen inventory that accordingly has a bulk  $\delta\text{D}$  value of about  $-20\text{ ‰}$  rel SMOW, or 160 ppm. Earth's D/H ratio is much higher than that of the outer atmospheres of gas giants that are as low as  $\sim 20$  ppm. This difference is commonly attributed to atmospheric loss of terrestrial protium over geologic time, a mechanism that provides a convenient partial explanation for Earth's high oxidation state. In fact, the D/H ratios of planets correlate with their mass, suggesting that deep levels in the gas giants have much higher D/H than their outer atmospheres (Figure; data from [3] but Uranus and Neptune are uncertain). If so, Earth's D/H ratio may be the best representative of the primitive solar system value.

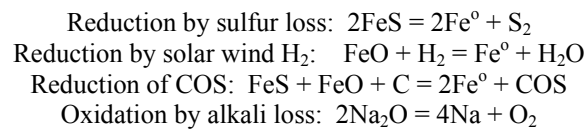
Oxygen isotope relations are codified in a "three-isotope" plot of  $\delta^{17}\text{O}$  vs.  $\delta^{18}\text{O}$  values. On this diagram, individual planets and meteorite types define striking parallel line segments whose 1) slope of  $\sim 0.53$  is the theoretical mass-dependent fractionation trend; 2) y-intercept is the  $\Delta^{17}\text{O}$  parameter; 3) center of mass is the bulk isotopic composition of the planet or family, and 4) length defines the extent to which the body or family has been fractionated into various reservoirs of disparate composition. Of these characteristics, the mass-dependent slope is best understood and, for three isotopes of any element having masses of  $m_1$ ,  $m_2$  and  $m_3$ , is precisely equal to:  $m_3(m_2-m_1)/(m_2(m_3-m_1))$  [ref 4]. The  $\Delta^{17}\text{O}$  value indicates the relative position of the lines and tends to increase with the K/U ratio and other ratios of volatile and refractory elements, likely representing a combination of chemical controls such as heliocentric distance and time of initial condensation. Segment length primarily reflects the effect of secondary fractionation processes, and would be enhanced by low T and by interactions of solids with liquids or gas; samples with high  $\delta^{18}\text{O}$  values commonly have high water contents. Earth is most highly fractionated, due to its protracted igneous evolution, low surface temperature, and the extensive interactions of its dynamic lithosphere with its large hydrosphere.



**References:** [1] Taylor H.P. and Sheppard S.M.F. (1986) *Rev. Mineral.*, 16, 227-271. [2] Gregory R.T. et al. (1989) *Chem. Geol.*, 75, 1-42. [3] Lodders K and Fegley B. (1998) *The Planetary Scientist's Companion*, Oxford University Press, 371 p. [4] Criss R.E. (1999) *Principles of Stable Isotope Distribution*, Oxford University Press, 254 p.

**REDOX STATE OF THE MOON'S INTERIOR.** J. W. Delano, Dept. of Earth and Atmospheric Sciences, and Dept. of Chemistry, The University at Albany (SUNY), Albany, NY 12222 jdelano@atmos.albany.edu

The redox state of the lunar interior is constrained by analyses of endogenous melts that have ascended to the lunar surface from depths of at least 400 kilometers. Lunar volcanic rocks (i.e., crystalline mare basalts and picritic volcanic glasses) are characterized by low oxidation states (i.e., ~1-2 log-units below the iron-wustite (IW) buffer [e.g., 1-15]), as indicated by the presence of Fe-rich metal [e.g., 4], occurrence of  $Ti^{3+}$  in armalcolite [e.g., 7,11,16], the high abundance of Cr, and the inferred dominance of Cr in the  $Cr^{2+}$  valence state [e.g., 12]. While it is considered likely that the observed redox states of lunar volcanic rocks and lunar volcanic glasses reflect the redox state of the Moon's interior, suggestions have been made that near-surface processes during eruption may have imposed late-stage overprints on the oxidation states that cause the observed redox states to differ from that of the Moon's interior. Open-system processes that have been suggested as having altered the original, pre-eruptive redox states of the lunar magmas during eruption include reduction by 'oxygen pumping' [e.g., 2,8,9], reduction by sulfur loss [e.g., 5,13,17,18], reduction by addition solar wind  $H_2$  from regolith [e.g., 19], reduction by carbon at low pressure [e.g., 15], reduction of loss of carbonyl sulfide, COS [e.g., 15], and oxidation by alkali loss [e.g., 9].



Current views are that the observed redox states of lunar volcanic samples are either due to (a) equilibrium between a Fe-rich metal phase (e.g., metallic core) and Fe-rich silicates (e.g., mantle), or (b) buffering by C-CO-CO<sub>2</sub>.

The observation that high P,T melting experiments on lunar magmatic compositions remained chemically unchanged when contained in high-purity Fe capsules [e.g., 20] is consistent with the former view. In addition, if lunar picritic glasses originated from source regions at pressures ~20 kbars (~2 GPa) in the Moon [e.g., 21-23], the pressure-dependence of the C-CO-CO<sub>2</sub> buffer would cause the redox state at those pressures in the Moon to be ~1.5 log-units fO<sub>2</sub> above the iron-wustite buffer. The consequence of that oxidation state, if picritic magmas were saturated with a Cr-rich spinel phase in the source-region

mineral residues, would be that the Cr abundances in the primary magmas would be ~2500 ppm, instead of the observed ~4000 ppm. The high Cr abundances in lunar picritic glasses and mare basalts (~4000 ppm) are consistent with their having originated at high pressures (~2 GPa) at a redox state of ~1-2 log-units fO<sub>2</sub> below the iron-wustite buffer, if those magmas were saturated with a Cr-rich spinel in their source-regions [e.g., 24-26].

These two chemical processes (i.e., metal/silicate equilibrium; C-CO-CO<sub>2</sub> buffer) that have been proposed for controlling the oxidation state of the Moon's interior deserve closer scrutiny. Their implications for the redox state of the deep lunar interior are significantly different.

- References:**
- [1] Smith J. V. et al. (1970) P A11 LSC, 897-925. [2] Bailey J. C. et al. (1970) P A11 LSC, 169-194. [3] Tuthill R. L. and Sato M. (1970) GCA, 34, 1293-1302. [4] El Goresy A. et al. (1971) PLSC 2<sup>nd</sup>, 219-235. [5] Sato M. and Hickling N. L. (1973a) LS IV, 650-652. [6] Lindsley D. H. et al. (1974) PLSC 5<sup>th</sup>, 521-534. [7] Kesson S. E. and Lindsley D. H. (1975) PLSC 6<sup>th</sup>, 911-920. [8] Biggar G. M. et al. (1971) PLSC 2<sup>nd</sup>, 617-643. [9] O'Hara M. J. et al. (1970) P A11 LSC, 695-710. [10] Usselman T. M. and Lofgren G. E. (1976) PLSC 7<sup>th</sup>, 1345-1363. [11] Stanin F. T. and Taylor L. A. (1980) PLPSC 11<sup>th</sup>, 117-124. [12] Schreiber H. D. and Haskin L. A. (1976) PLPSC 7<sup>th</sup>, 1221-1259. [13] Brett R. (1976) GCA, 40, 997-1004. [14] Sato M. (1976) PLSC 7<sup>th</sup>, 1323-1344. [15] Sato M. (1979) PLPSC 10<sup>th</sup>, 311-325. [16] Wechlser B. A. et al. (1975) LS VI, 860-862. [17] Gibson E. K., Jr. and Moore G. W. (1974) PLSC 5<sup>th</sup>, 1823-1837. [18] Gibson E. K., Jr. et al. (1975) PLSC 6<sup>th</sup>, 1287-1301. [19] Mao H. K. et al. (1974) PLSC 5<sup>th</sup>, 673-683. [20] Kesson S. E. and Lindsley D. H. (1976) Geophys. Space Phys., 14, 361-373. [21] Elkins L. T. et al. (2000) GCA, 64, 2339-2350. [22] Delano J. W. (1980) PLPSC 11<sup>th</sup>, 251-288. [23] Shearer and Papike J. J. (1993) GCA, 57, 4785-4812. [24] Barnes S. J. (1986) GCA, 50, 1889-1909. [25] Delano J. W. (2001) Origin Life Evol. Biosphere, 31, 311-341. [26] Roeder P. L. and Reynolds I. (1991) J. Petrol., 32, 909-934.

**HOW DID THE TERRESTRIAL PLANETS ACQUIRE THEIR WATER?** M. J. Drake, M. Stimpfl, and, D. S. Lauretta, Lunar and Planetary Laboratory, University of Arizona, Tucson, Arizona 85721-0092, U.S.A. drake@lpl.arizona.edu

**Introduction:** There is no consensus on the origin of water in the terrestrial planets. Earth demonstrably has water. Odyssey has shown vast water ice sheets buried under a thin layer of dust polewards of about 60° of latitude in both hemispheres of Mars [1]. The D/H ratio of Venus is about 100 times that of Earth's oceans [2], and is plausibly explained by loss of H<sub>2</sub>O through UV photodissociation at the top of the Venus atmosphere. Mercury and the Moon appear to be bone dry, possibly due to volatile loss in giant impacts.

**Sources of water:** It has generally been thought that the accretion disk was too hot at 1 AU for hydrous minerals to be stable, although the thermal history of the inner disk is based on models, not observations. Comets had been a popular choice for the source of water, as they demonstrably contain water ice. However, the measured D/H ratios in Hale-Bopp, Hyakutake, and Halley are identical within error and, if these measurements are representative of bulk comets, they constrain the contribution of cometary water to less than 15%. The ratio of Ar/H<sub>2</sub>O in comet Hale-Bopp and Ar/O in comet LINEAR imply still lower limits on cometary water if the spectral measurements are reliable. Asteroids are dynamically plausible sources of water, but Os isotopes in Earth's mantle rule out known meteorite types as the source of Earth's water. See Drake and Righter [3] for a more thorough discussion. Inward migration of phyllosilicates has also been proposed [4].

**Indigenous source revisited:** Let us accept for now that the inner accretion disk was too hot for hydrous minerals to be stable and consider an alternative source of H<sub>2</sub>O. The dust in the disk was bathed for some time in a sea of H and O. The amount of water vapor present in the accretion disk within 3 A.U. equaled about three times the Earth's mass [5].

**Adsorption:** It is possible that water from the gas phase could be adsorbed onto grains in the inner solar system and subsequently accreted into the terrestrial planets. Stimpfl *et al.* [6] modeled the adsorption of water from 1500K to 1000K using a Monte Carlo simulation with a grid of 10000 adsorption sites, and an iterative process allowing the surface to reach steady state saturation at each temperature. Water molecules not only interact with the substrate by means of weak bonds (~5kJ/mole) but also establish hydrogen bonds with other water molecules present in a monolayer [7]. The energy of the incoming molecules was computed using the Maxwell-Boltzmann probability distribution. We allowed only for the adsorption of one monolayer, neglected porosity and surface roughness, considered water an

infinite reservoir, and assumed that all the particles interacting with the surface were water molecules.

We pulverized the Earth into homogenous spheres of 0.1 m radius. The adsorbed water potentially stored in the dust corresponds to ~3 times the Earth's oceanic + atmospheric + crustal water (OAC) [8] and ~1.5 times the Earth's OAC + mantle water [8]. If the grain size increases, however, the amount of water adsorbed on the surface decreases; in this model the biggest grain size that allows for 1 Earth's OAC water to be adsorbed is ~ 0.3 m. On the other hand, porosity and surface roughness would increase the number of adsorption sites as well as shelter adsorbed molecules from bombardment.

**Non-mineral bonding:** Ab initio calculations at 0°K in which the Gibbs free energy of Si – O clusters is minimized and then a H<sub>2</sub>O molecule is introduced indicate that strong chemical bonds can be formed between the water molecule and the Si – O cluster [9], making retention of H<sub>2</sub>O during the later violent stages of accretion more likely. These calculations need to be conducted at realistic nebular temperatures.

**Conclusions:** These considerations suggest that H<sub>2</sub>O may have been obtained by the terrestrial planets directly from the gas phase in the accretion disk. The initial water budgets would be functions of P and T and, hence, heliocentric distance. Accretion of water in the presence of metal will lead to extraction of H into planetary cores and progressive oxidation of planetary mantles [10, 11]. The “feeding zones” of the terrestrial planets would be relatively narrow over most of planetary accretion, consistent with differences in O-isotopes, Cr-isotopes, and major element compositions of Earth and Mars [3]. The “late veneer” could plausibly be of asteroidal origin, consistent with dynamical calculations [8].

**References:** [1] Boynton W.V. *et al.* (2002) *Science* **297**, 81-85. [2] Donahue T.M. and Pollack J.B. 1983) In *Venus*, U of A Press, 1003-1036. [3] Drake M.J. and Righter K. (2002) *Nature* **416**, 39-44. [4] Ciesla F.J. *et al.* (2004) LPSC XXXV, abstract 1219. [5] Lécluse C. and Robert F. (1994) *Geochimica et Cosmochimica Acta* **58**, 2927-2939. [6] Stimpfl M. *et al.* (2004) *MAPS* **39** (in press). [7] de Leeuw N.H. *et al.* (2000) *Phys. Chem. Min.* **27**, 332-341. [8] Morbidelli A. *et al.* (2000) *MAPS* **35**, 1309-1320. [9] Gibbs G. (2004), personal communication. [10] Drake M.J. (2003) *GCA* **67**, A83. [11] Righter K. (2004) LPSC XXXV, abstract 1674.

**MOLECULAR OXYGEN MIXING RATIO AND ITS SEASONAL VARIABILITY IN THE MARTIAN ATMOSPHERE.** C. England<sup>1</sup> and J. D. Hrubes<sup>2</sup>, <sup>1</sup>Jet Propulsion Laboratory, 4800 Oak Grove Dr., Pasadena, CA 91109, cengland@jpl.nasa.gov, <sup>2</sup>Raytheon Polar Services, Amundsen-Scott South Pole Station, cusplab@usap.gov.

**Abstract:** The mixing ratio of molecular oxygen and other species that do not condense at martian ambient conditions will vary as the mass of atmosphere oscillates over a martian year due to alternate condensation and vaporization of carbon dioxide at the poles [1]. This variation can be estimated utilizing measurements of mixing ratio made *in-situ* together with multi-year measurements of atmospheric pressure, both available from the Viking landers starting in 1976. The concentration of non-condensables, on average, will be approximately an inverse function of the atmospheric pressure.

Viking Lander 1 (VL1) measured atmospheric pressure at the surface of Mars at 22.3° north latitude and 48.0° longitude for approximately 3½ martian years [2]. Three *in-situ* measurements for molecular oxygen are reported, all from the Viking landers. The first was from the neutral mass spectrometer (NMS) during VL1's entry, measured at 135 km, providing a mixing ratio of 0.003, or 0.3% [3]. The other two determinations were from VL1's gas chromatograph/mass spectrometer. Both were reported as unreliable but as bracketing the mixing ratio of molecular oxygen between 0.1%-0.4% [4]. No values were reported from instruments on Viking Lander 2.

A later summary [5] provided an estimate of atmospheric composition at the martian surface, suggesting a mixing ratio for oxygen of 0.13%, a value that is very often cited as the accepted value [1,6]. This value, however, appears to have its origin from two Earth-based measurements made prior to the Viking mission, and might be considered less dependable than the VL1 NMS *in-situ* measurement [5,7,8].

Figure 1 plots the mixing ratio of molecular oxygen over a full martian year by inverse scaling with the atmospheric pressure, and by utilizing the VL1 entry value (0.3%) and date of entry (areocentric longitude of 97.04°). This relationship is implied by the expected near-exclusion of molecular oxygen and other low-boiling species in the condensed phase at the poles.

The highest molecular oxygen concentration is 0.34%, occurring at the period of lowest atmospheric pressure and smallest atmospheric mass at an areocentric longitude of about 145°. This value is markedly higher than the commonly cited value of 0.13%, and may suggest additional analysis is warranted to understand the compositional behavior of the martian at-

mosphere. The smallest predicted concentration is 0.25% at about 261°.

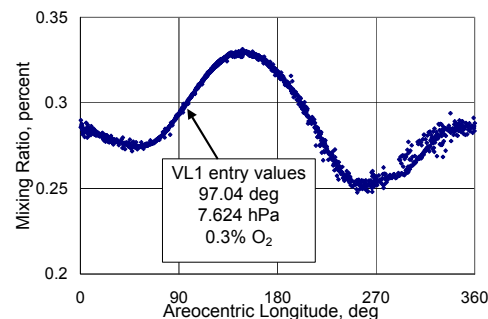


Fig. 1. Seasonal Variation of Mixing Ratio of O<sub>2</sub>

Other non-condensing species will experience similar variation that can be estimated by simple proportions. Carbon monoxide, an important compound in the understanding of martian atmospheric chemistry, has not yet been measured *in-situ*, and its mixing ratio remains highly uncertain.

Figure 1 illustrates the global average mixing ratio of oxygen since the amount of non-condensing species will vary locally as they are selectively concentrated and then expelled from the poles during the condensation-sublimation cycle. While it can be argued that the measurement for molecular oxygen at 135 km may not be fully representative of surface concentration, Figure 1 assumes no significant differentiation of neutral species is likely at the fractional percent level. If oxygen is present at the levels suggested, direct extraction from the martian atmosphere for use as a propellant for sample or crew return as well as for breathing may be practical [9].

**References:** [1] Kieffer, H.H. et al (1992) *Mars*, Kieffer H.H. et al, U. Ariz. Press, 1-33. [2] *NASA Planetary Data System*, file vl\_avep\_dat.txt. [3] Nier, A. O. et al (1976) *Science*, 193, 786-788. [4] Owen, T. and Biemann, K. (1976) *Science*, 193, 801-803. [5] Owen, T. et al, *JGR*, 82, 4635-4639. [6]. see for example Dauphas, N. (2003) *ICARUS*, 165, 326-339. [7] Barker, E.S. (1972) *Nature*, 238, 447-448. [8] Carlton, N.P and Traub W. A. (1972) *Science*, 177, 988-992. [9] England, C. and Hrubes, J.D. (2001) *MARRS-Mars Atmosphere Resource Recovery System*, study report available at <http://www.niac.usra.edu>.